Effect of the Position and the Number of Broken Bars on Asynchronous Motor Stator Current Spectrum

Arezki Menacer*, Sandrine Moreau**, Abdelhamid Benakcha *, Mohamed Said Naît Saïd ***

* LGEB. Laboratoire de Génie Electrique de Biskra, Université Med Khider B.p 145, 07000, Biskra, Algérie
** LAII. Laboratoire d'Automatique et d'Informatique Industrielle, 40, av. du Recteur Pineau 86022 Poitiers cedex France
*** LSPIE. Laboratoire de l'université de Batna, rue Med El Hadi Boukhlouf 05000 Batna, Algérie

Abstract— **The asynchronous motor has an interest in strong powers applications requiring speed variation. Even if it is robust, it is not saved by electrical or mechanical defects.**

Among rotor defects, we can quote a fissure or a total break of bar, a rupture of end ring circuit, an eccentricity of the rotor axis...

In this paper, we use a technique based on the spectral analysis of stator current in order to detect a breakdown or a defect in the rotor. Thus, the number and the position effect of the breaks have been highlighted.

The effect is highlighted by considering the machine supplied directly through a balanced three-phase network.

Index Terms- broken rotor bar, asynchronous motor, modeling, diagnosis, stator current spectrum.

I. INTRODUCTION

Although the asynchronous machine is famous for its qualities of robustness and its low cost of construction, it happens nevertheless that it can present electrical or mechanical failures.

The developed techniques based on spectral signatures analysis of rotor defects (such as partial or total break of squirrel-cage bars or of end ring portion) and stator defects (such as short-circuits) must detect early failure. So from the signatures analysis of the defect, the stop of the production process line, where the asynchronous motor is used, can be programmed to replace the failing elements before the breakdown becomes very serious.

The early diagnosis of defects is of importance and mobilizes researchers in electrical engineering, automatic and signal processing fields.

Among rotor defects which can appear, there is the break of rotor bars or of an end ring portion. The problem is that direct measurement of rotor variables is difficult for a squirrel-cage asynchronous motor.

The consequences of these defects may be the following ones:

- a mechanical ageing of the rotor axis because of the torque fluctuations,
- higher risks of the adjacent bars break because of high currents and, consequently, significant electrodynamics constraints,
- waveform distortions of the machine supply and therefore of the electric network.

We can also quote other defects types such as:

A. Internal defects

The internals defects can concern the stator or the rotor:

STATOR DEFECTS

The stator is rather subjected to electric stresses which can be accompanied by the following defects:

- short-circuit in the whorls of the same phase,
- short-circuit between phases,
- cut in the phase,
- defect in the magnetic circuit (sheet rupture),
- defect in the sheet insulation,
- electrical defect of insulation in the stator windings,
- ageing of insulators.

ROTOR DEFECTS

Among these defects we can quote:

- misalignment of the rotor in consequence of a wear of the bearings detectable by the monitoring of the vibrations or the current [1],
- break of one or several bars,
- break of end rings,
- defect of the magnetic circuit.

B. External Defects

These defects may have different origins:

- electrical: the transitory mode or the unbalance of the feeding,
- thermals: operating temperature elevation, hot points, overload,
- mechanical: frictions, shocks in service,…
- chemical: corrosion, moisture.

In particular, outgoing research work is currently concentrated on rotor bar faults and on the development of diagnosis techniques applied to three-phase squirrel-cage induction machines [2]–[4].

II. Model of the Three Phase Asynchronous Motor

The model of the asynchronous motor takes into account the following assumptions [5]:

- the saturation and the skin effect are negligible,
- the air-gap is uniform,
- the mmf distribution in the air-gap is sinusoidal,
- the rotor bars are isolated from the magnetic circuit of the rotor,
- the relative permeability of the magnetic circuit is supposed to be infinite.

Although the mmf of the stator windings is supposed to be sinusoidal, other distributions of rolling up could also be considered by simply employing the superposition theorem. It is justified by the fact that the different components of the space harmonics do not act the ones on the others [6].

In order to study the phenomena taking place in the rotor, the latter is often modeled by N_R meshes as shown on figure 1.

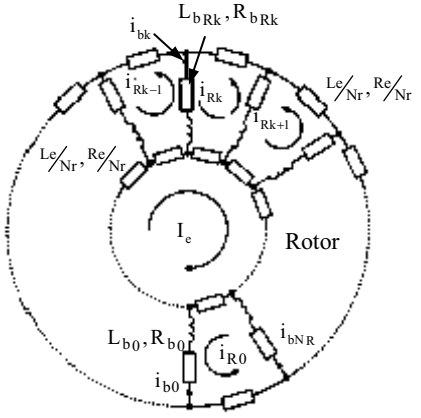

Fig. 1. Rotor cage equivalent circuit

The induction motor mathematical model can be written as follows:

$$[V]=[R][I]+\frac{d}{dt}([L][I]) \quad (1)$$

with: $[V]=\begin{bmatrix}[V_S]\\ [V_R]\end{bmatrix}$, $[I]=\begin{bmatrix}[I_S]\\ [I_R]\end{bmatrix}$

and:

$[V_S]=[V_{S1}\ V_{S2}\ V_{S3}]^t$, $[V_R]=[0\ 0\ 0\ \cdots\ 0]^t_{1\times(N_R+1)}$

$[I_S]=[I_{S1}\ I_{S2}\ I_{S3}]^t$,

$[I_R]=[I_{R1}\ ..\ I_{Rk}\ ..\ I_{RN_R}\ I_e]^t_{1\times(N_R+1)}$

The resistance global matrix can be written as:

$$[R]=\begin{bmatrix}[R_S]_{3\times3} & \vdots & [0]_{3\times N_R} & \vdots & [0]_{3\times1}\\ \cdots & \cdots & \cdots & \cdots & \cdots\\ [0]_{N_R\times3} & \vdots & [R_R]_{N_R\times N_R} & \vdots & -\frac{R_e}{N_R}[1]_{N_R\times1}\\ \cdots & \cdots & \cdots & \cdots & \cdots\\ [0]_{1\times3} & \vdots & -\frac{R_e}{N_R}[1]_{1\times N_R} & \vdots & R_e[1]_{1\times1}\end{bmatrix} \quad (2)$$

where: $[R_S]_{3\times3}=\begin{bmatrix}R_S & 0 & 0\\ 0 & R_S & 0\\ 0 & 0 & R_S\end{bmatrix}$

The global inductance matrix can be represented by:

$$[L]=\begin{bmatrix}[L_S]_{3\times3} & \vdots & [M_{SR}]_{3\times N_R} & \vdots & [0]_{3\times1}\\ \cdots & \cdots & \cdots & \cdots & \cdots\\ [M_{RS}]_{N_R\times3} & \vdots & [L_R]_{N_R\times N_R} & \vdots & -\frac{L_e}{N_R}[1]_{N_R\times1}\\ \cdots & \cdots & \cdots & \cdots & \cdots\\ [0]_{1\times3} & \vdots & -\frac{L_e}{N_R}[1]_{1\times N_R} & \vdots & L_e[1]_{1\times1}\end{bmatrix} \quad (3)$$

where:

$$[M_{SR}]_{3xN_R}=\begin{bmatrix}... & -M_{SR}\cos(\theta+k.a) & ...\\ ... & -M_{SR}\cos(\theta+k.a-\frac{2\pi}{3}) & ...\\ ... & -M_{SR}\cos(\theta+k.a-\frac{4\pi}{3}) & ...\end{bmatrix}, \quad k=0,N_R-1$$

$$a=p\frac{2\pi}{N_R}$$

$$[L_S]_{3\times3}=\begin{bmatrix}L_{Sp} & M_S & M_S\\ M_S & L_{Sp} & M_S\\ M_S & M_S & L_{Sp}\end{bmatrix}$$

The detailed expressions of $[R_R]_{N_R\times N_R}$ and $[L_R]_{N_R\times N_R}$ are respectively the following ones:

$$[R_R]_{N_R\times N_R}=\begin{bmatrix}R_{b0}+R_{b(N_R-1)}+2\frac{R_e}{N_R} & -R_{b0} & 0 & \cdots & \cdots & \cdots & -R_{b(N_R-1)}\\ 0 & \cdots & -R_{b(k-1)} & R_{bk}+R_{b(k-1)}+2\frac{R_e}{N_R} & -R_{bk} & 0\ \cdots & 0\\ -R_{b(N_R-1)} & 0 & \cdots & \cdots & 0 & -R_{b(N_R-2)} & R_{b(N_R-1)}+R_{b(N_R-2)}+2\frac{R_e}{N_R}\end{bmatrix}$$

$$[L_R]_{N_R \times N_R} = \begin{bmatrix} L_{Rp}+2L_b+2\frac{Le}{N_R} & M_{RR}-L_b & M_{RR} & M_{RR} & \cdots & M_{RR}-L_b \\ M_{RR}-L_b & L_{Rp}+2L_b+2\frac{Le}{N_R} & M_{RR}-L_b & M_{RR} & M_{RR} & \cdots \\ M_{RR} & M_{RR}-L_b & L_{Rp}+2L_b+2\frac{Le}{N_R} & M_{RR}-L_b & M_{RR} & \cdots \\ M_{RR} & \vdots & \ddots & \ddots & \ddots & \ddots \\ \vdots & \ddots & \ddots & \ddots & \ddots & \ddots \\ M_{RR}-L_b & M_{RR} & M_{RR} & \cdots & M_{RR}-L_b & L_{Rp}+2L_b+2\frac{Le}{N_R} \end{bmatrix}$$

III. Defect Model of the Motor

In order to simulate the defect of bar break, a defect resistance R_{bF} is added to the corresponding element of the rotor resistance matrix R_R [7]:

$$[R_F]_{N_R x N_R} = \begin{bmatrix} 0 & \cdots & 0 & \cdots & \cdots & 0 \\ \vdots & \cdots & \vdots & \vdots & \cdots & \vdots \\ \vdots & \cdots & 0 & 0 & \cdots & 0 \\ 0 & 0 & R_{bF_k} & -R_{bF_k} & 0 & 0 \\ 0 & 0 & -R_{bF_k} & R_{bF_k} & 0 & 0 \\ \vdots & \vdots & 0 & 0 & \vdots & \vdots \\ \vdots & \vdots & \vdots & \vdots & \vdots & \vdots \end{bmatrix}$$

Consequently, the squirrel cage resistance matrix, taking into account the defect, is defined by:

$$[R_{RF}]_{N_R x N_R} = [R_R]_{N_R x N_R} + [R_F]_{N_R x N_R}$$

The mechanical equations must also considered:

$$\frac{d}{dt}\omega = \frac{1}{J_m}(Ce - Cr) \qquad (4)$$

with: $$\omega = \frac{d\theta}{dt}$$

The application of the classical Park's transformation to the three-phase stator currents allows calculating the stator currents I_{ds} and I_{qs} and leads for the following torque expression:

$$Ce = \sqrt{\frac{3}{2}}\, p\, M_{SR}\left\{ I_{qS} \sum_{k=0}^{N_R-1} I_{Rk+1} \cos(k.a) - I_{ds} \sum_{k=0}^{N_R-1} I_{Rk+1} \sin(k.a) \right\} \qquad (5)$$

IV. Simulation Results and Discussions

After several transformations, the model of the asynchronous motor is given by expressions (1) to (5).

The classical Fast Fourier Transform (FFT) is used to realize the frequency analysis of the measured stator phase currents in order to determine the spectral signatures of the defect [8].

The spectral analysis of stator phase currents highlights the effect of the defect through the appearance of harmonics around the fundamental [9]-[11]

Their amplitudes increase according to the number of defective bars at characteristic frequencies (equation (6)), [12, 13].

$$f_{defect} = (1 \pm 2.n.g)fs\,, \qquad n=1,2,.. \qquad (6)$$

where f_{defect} are the sideband frequencies associated with the broken rotor bar and where g represents the motor slip and fs the stator frequency.

A. *Effect of the break severity on the stator current spectrum*

To highlight the effect of the break severity, we simulate bars break by increasing the broken bar resistance from 10 R_b to 100 R_b.

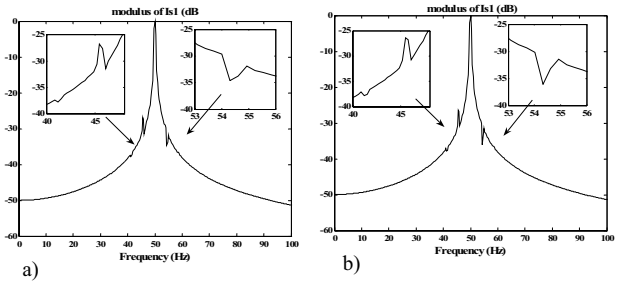

Fig. 2. Stator current spectrum analysis for an increase of the broken bar resistance (g =3.6%) a) 10 Rb b) 100 Rb

It is noticed that the value of the broken bars resistance introduces a modification on the stator current spectrum: harmonics appears on both sides of the fundamental and they verify the equation (6). (figures 2-a and 2-b)

B. *Effect of the number and the position of broken bars*

We consider the several bars breaks defect so as to take into account their number and their position.

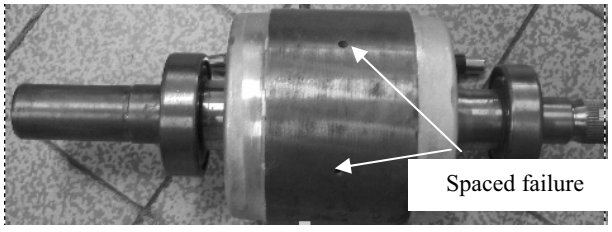

Fig. 3. Example of spaced broken bars

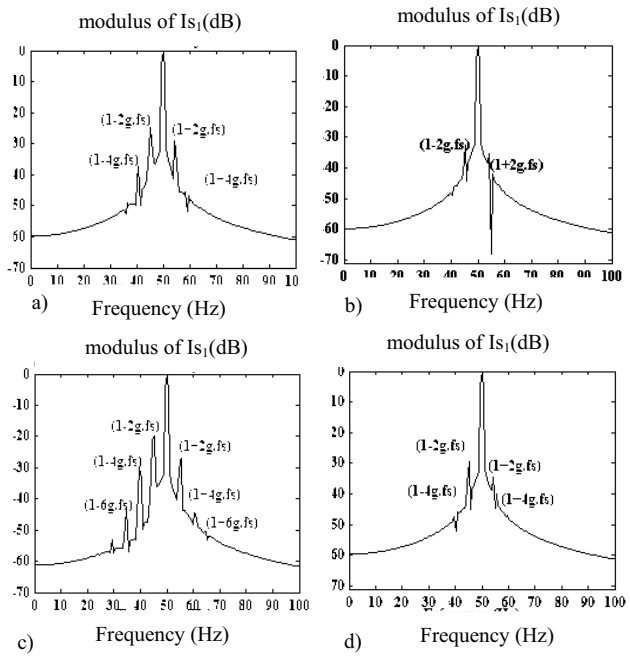

Fig. 4. Stator current spectrum taking into account the number and the position of the broken bars (g=3.6%):
a) Adjacent two break bars b) Spaced two break bars c) Adjacent three break bars d) Spaced three break bars

On the figure (4), we notice the appearance of harmonics on the spectrum. These harmonics have amplitude which increases according to the raise of the defective bars number and changes with their positions. Table 1 highlights the influence of the number and the position of broken bars on the stator current spectrum.

The frequencies values given by the equation (6) and those deduced from the spectrum graphs are in agreement with one another for different types of breaks [14]. The 3rd and the 4th harmonic do not appear on the spectrum because there is compensation due to the relative position of the broken bars (cylindrical symmetry).

The increase of the harmonics amplitude is due to the increase of the broken bars number. The amplitude of the lines increases with the number of broken adjacent bars. Moreover, the six lines correspond to the defect which appears.

C. *Effect of the load on the stator current spectrum*

The effect of the load on the stator current spectrum is highlighted by considering a break of three adjacent bars with different slips (g= 0.001 %, g=1.15 %, g=2.3 % and g=3.6 %)(see figure (5)).

We notice a tightening of harmonics spectrum for weak slips. The spectral analysis of signals becomes then delicate in this case.

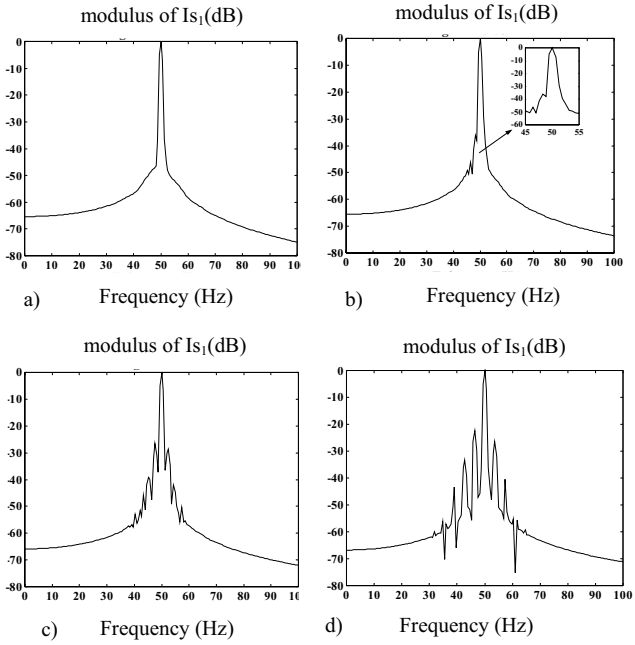

Fig.5. Stator current spectrum with different slips for adjacent three break bars: a) g= 0.001% b) g=1.15% c) g=2.3 % d) g=3.6 %

So it appears from figure. 5 that the defect is better highlighted when the machine is charged.

TABLE.I
FREQUENCIES AND MAGNITUDES OF THE STATOR CURRENT SPECTRUM:
a) Adjacent two break bars b) Spaced two break bars c) Adjacent three break bars d) spaced three break bars

The number and the position of broken bars		f_{cal}=(1-6g)fs **line 1**	f_{cal}=(1-4g)fs **line 2**	f_{cal} =(1-2g)fs **line 3**	f_{cal}=(1+2g)fs **line 4**	f_{cal}=(1+4g)fs **line 5**	f_{cal}=(1+6g)fs **line 6**
a)	$f_{calculated}$ (Hz)	35.94	40.62	45.31	54.68	59.37	64.05
	$f_{deduced}$ (Hz)	36.58	40.87	45.11	54.33	58.57	63.54
	Magnitude (dB)	-49.16	-37.60	-24.91	-29.31	-45.6	-50.9
b)	$f_{calculated}$ (Hz)	36.26	40.84	45.42	54.57	59.15	63.73
	$f_{deduced}$ (Hz)	/	39.64	45.12	54.27	/	/
	Magnitude (dB)	/	-48.36	-32.71	-35.40	/	/
c)	$f_{calculated}$ (Hz)	34.576	39.71	44.85	55.14	60.28	65.42
	$f_{deduced}$ (Hz)	34.774	39.67	45.09	55.47	60.40	64.72
	Magnitude (dB)	-43.479	-30.46	-20.08	-27.00	-44.65	-50.81
d)	$f_{calculated}$ (Hz)	35.636	40.42	45.21	54.78	59.57	64.36
	$f_{deduced}$ (Hz)	/	40.83	45.137	54.15	59.79	/
	Magnitude (dB)	/	-46.02	-29.77	-34.85	-47.25	/

D. *Effect of the broken bars position on the current spectrum*

In these cases, we consider two broken bars and we define α angle position between two broken bars.

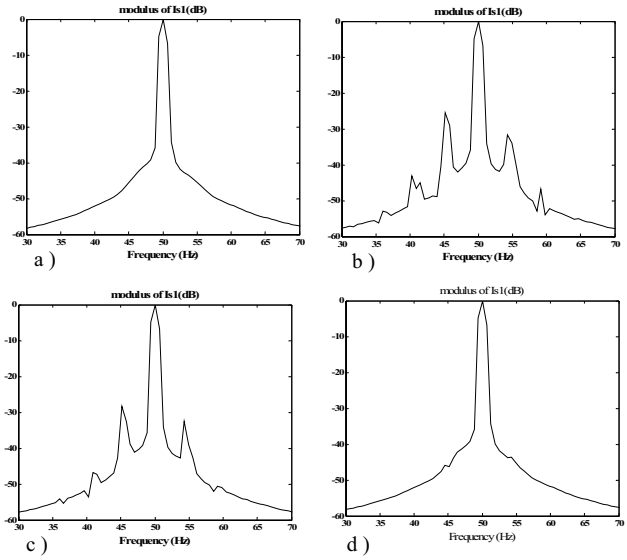

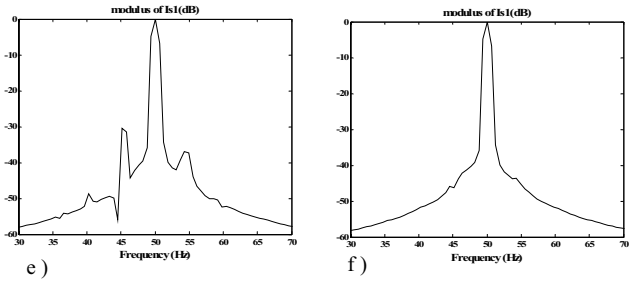

Fig. 6. Stator current spectrum with different position of the two broken bars: a) healthy motor b) α =22,5° c) α =45° d) α =90° e) α =135° f) α =180°

If the broken bars are close to one another (figure 6b, 6c), the amplitude of the harmonics located on both sides of the fundamental are significant (table 2). On the other hand, if the angle α is equal to 90° or to 180° (figure 6d, 6f), the amplitude of the harmonics are weak and it is difficult to distinguish the healthy machine from the defective one (figure 6a).

TABLE.II
Effect of broken bars position on the current spectrum

		$\alpha = 22.5^{\circ}$	$\alpha = 45^{\circ}$	$\alpha = 90^{\circ}$	$\alpha = 135^{\circ}$	$\alpha = 180^{\circ}$
Lower	f (Hz)	54.2857	54.2857	54.2857	54.2857	54.2857
		59.1705	59.1705	/	58.9862	/
		64.6083	/	/	/	/
	Magnitude (dB)	-31.6228	-32.4196	-43.5965	-36.8860	-43.5380
		-46.7325	-50.6360	/	-50.2193	/
		-55.0658	/	/	/	/
Upper	f (Hz)	45.1613	45.1613	44.5161	45.2535	44.6083
		40.2765	40.9217	/	40.2765	/
		36.0369	36.1290	/	36.4977	/
	Magnitude (dB)	-25.8699	-28.2237	-45.9357	-30.4825	-45.8772
		-43.0629	-46.8494	/	-48.9035	/
		-52.5804	-54.1155	/	-54.0789	/

V. CONCLUSION

This paper presents within the framework of the diagnosis the asynchronous motor broken bars simulation based on the development of a multi windings model.

The stator current spectrum analysis shows the presence of a defect due to the break or the rupture of bars thanks to the appearance of different harmonics given by the equation (6).

The severity of the defect can be deduced from the amplitude variation of the harmonics located on both sides of the fundamental.

Broken bars position and number effect result in an increase of harmonics amplitude in respect to the number of broken bars. The break of adjacent bars appears very well on the stator current spectrum. Generally, we noticed that the influence of the rotor defect on the stator current spectrum is much more visible if the distance between two broken bars is larger.

However, when the position of two broken bars is equal to 90° or 180°, it is difficult to distinguish from the current spectrum analysis the healthy case from the defective one.

The effect of the load can be resumed as follows:

- a weak slip (g) results in a contracting of the harmonics interval,

- a significant g (full load) results in an expansion of the harmonics interval and an increase of the harmonics amplitude.

So the severity of the defect can be deduced from the amplitude of harmonics.

And the interval between these harmonics becomes broader if the machine is at full load. However the variation of the slip can induce in error because it causes

the appearance of additional harmonics (figure 5). So we can note that the slip is a significant parameter to take into account for the diagnosis of asynchronous motors, particularly for rotor defects detection.

LIST OF SYMBOLS

Pn	output power	1.1 kW
Vs	stator voltage per phase	220 V
fs	stator frequency	50 Hz
p	poles pair number	1
R_S	stator resistance	7.58 Ω
R_{b0}	rotor bar resistance	0.15mΩ
R_e	resistance of end ring segment	0.15mΩ
L_{b0}	rotor bar inductance	0.1µH
L_e	inductance of end ring	0.1µH
L_{sf}	leakage inductance of stator	0.0265H
M_{sr}	mutual inductance stator rotor	46.422mH
N_R	number of rotor bars	16
N_S	number of turns per stator phase	160
J_m	inertia moment	0.0054 Nms^2
Rb_{FK}	additional resistance of a defect rotor bar	
a	electrical angle of two rotor adjacent meshs	0.392
θ	angle between stator phase 1 and od axis	
g	slip	
f cal	frequencies calculated	
id_S, iq_S	Park's currents	
α	angle position between two broken bars.	

REFERENCES

[1] William R. Finlley, Mark M. Hodowanec, "An analytical approach to resolving motor vibration problem", *IEEE* 1999, p. 217-232.

[2] N. M. Elkasabgy and A. R. Easthem, "Detection of broken bars in the cage rotor on an induction machine," *IEEE Trans. Ind. Applicat.*, Vol. 28, pp. 165–171, Jan./Feb. 1992.

[3]] M. E. H. Benbouzid, "Bibliography on induction motors faults detection and diagnosis," *IEEE Trans. Energy Conversion*, Vol. 14, pp. 1065–1074, Dec. 1999.

[4] D. Kostic-Perovic, M. Arkan, and P. Unsworth, "Induction motor fault detection by space vector angular fluctuation," in *Conf. Rec. IEEE-IAS Annu. Meeting*, vol. 1, 2000, pp. 388–394.

[5] H. Razik,H. Henao and R. Carlson, " The Effect of Inter -bar Currents on the Diagnostic of the Induction Motor", 2004 IEEE pp 797-802.

[6] A. R. T. A. Lipo , "Complex vector model of the squirrel-cage induction machine including instantaneous rotor bar currents" , *IEEE Transaction on Industry Application*, Vol.35, N°6, Nov/Dec 1999.

[7] A. Abed, L. Baghli, H.Razik, A. Rezzoug , "Modeling induction motors for diagnosis purposes", *EPE' 99 Lausanne.*

[8] M. Artioli, A. Yazidi, F. Filippetti, G.A. Capolino, "A general purpose software for signal processing oriented to the diagnosis of electrical machines," *Proceedings of IEEE International Symposium on Industrial Electronics Conference (ISIE'04)*, Ajaccio (France), May 2004, Vol. 2, pp.809-814.

[9] A. Menacer, M. S. Nait Said, A. Benakcha, S. Drid, "Stator current analysis of incipient fault into asynchronous motor rotor bars using Fourier fast transform", *Journal of* Electrical *Engineering, Slovakia*, Vol. 5-6, 2004,pp 122-130

[10] A. Menacer, M. S. Nait Said, A. Benakcha, S. Drid, "Détection d'une Cassure de Barre Rotorique d' un Moteur Asynchrone par Analyse Spectrale du Courant Statorique", *CNGE'2004, première Conference nationale sur le génie électrique* 29/11/-01/12 2004 , pp 261-265, université Ibn Khaldoun Tiaret – Algérie

[11] A. Abed, L., E. Weinachter, A.Razik, A. Rezzoug ,"Real time implementation of the Sliding DFT Applied to on line's broken bars diagnostic", *IEEE International Electric machines and drives Conference, IEMDC'2001, Cambridge, MA USA,* June17, 20, 2001, p. 345-34

[12] M Benbouzid, "A Review of induction motors signature analysis as a medium for fault detection", *IECON'98, Aachen ,* Germany, 1998, pp 1950-1955

[13] Bulent Ayhan,, Mo-Yuen Chow, and Myung-Hyun Song, "Multiple Signature Processing-Based Fault Detection Schemes for Broken Rotor Bar in Induction Motors", *IEEE Transactions on Energy Conversion*, Vol. 20, N°. 2, June 2005.

[14] A. Menacer, M. S. Nait Said, A. Benakcha, S. Drid, "Stator Current Analysis of Incipient Fault into Induction Machine Rotor Bars", *Journal of Electrical Engineering*, Roumanie, Vol 4, Nº2–2004, pp 5-12.